Journal of Materials Chemistry B

Accepted Manuscript

This article can be cited before page numbers have been issued, to do this please use: P. Gaur, A. Kumar, S. bhattacharyya and S. Ghosh, *J. Mater. Chem. B*, 2016, DOI: 10.1039/C6TB00787B.

ROYAL SOCIETY OF CHEMISTRY

www.rsc.org/materialsB

View Article Online
DOI: 10.1039/C6TB00787B

Journal Name

ARTICLE

Biomolecular recognition at cellular level: geometrical and chemical functionality dependence of a low phototoxic cationic probe for DNA imaging

hReceived 00th January 20xx,
Accepted 00th January 20xx

DOI: 10.1039/x0xx00000x

www.rsc.org/

Pankaj Gaur,[a] Ajay Kumar,[b] Shalmoli Bhattacharyya,[b,*] and Subrata Ghosh[a,*]

A combined approach was adopted to understand the impact of structural geometry as well as suitable chemical functionality of a molecular probe for its efficient binding in the minor groove of DNA. Development of a small chemical library of different lutidinium conjugates (**P1-P5**), and molecular simulation using DFT calculations clearly demonstrated that the semilunar conformation of a molecular probe equipped with requisite chemical functionality is the key parameter for its proper binding in the minor groove of DNA. The comparative optical responses of these probes (**P1-P5**) coupled with the theoretical studies illustrated that only **P3** displayed considerable fluorescence enhancement in the presence of DNA because of its semilunar geometry and special chemical architecture. Furthermore, the bioassays clearly revealed that the probe can penetrate the cell membrane of the live as well as dead cells without the help of any permeabilization agent. The microscopic cellular imaging established that the probe **P3** can stain the nuclear region of the cells with high contrast and negligible cytoplasmic spillage without causing any cellular deterioration. The specificity and binding efficiency of **P3** toward DNA were established by performing DNase/RNase digest tests and gel electrophoresis experiment. Most importantly, **P3** exhibited minimum phototoxicity and high photobleaching resistance in cellular medium under continuous exposure of light source which are highly desirable for real time monitoring of many biological events. Altogether, the investigated properties of **P3** enlightened its admirable and persuasive standing as a cell-compatible, bright and photostable molecular probe for nuclear imaging in various bio-medical applications.

Introduction

Heterocyclic compounds have been known for their diverse biological and medicinal importance largely because of their inherent structural resemblance with naturally occurring bioactive compounds.[1-4] Moreover, geometrically well-defined fused polycyclic heterocycles gain structural specialization as bioactive templates such as drugs, inhibitors and fluorescent probes for imaging various biomolecules including DNA inside cellular systems.[5-7] The precise geometry and orientation are the key factors to be considered while designing them to ensure their specific interactions with deep and shallow minor groove of DNA. Because of its vitality in molecular biology, DNA is known as the blue print of life which not only controls the genetic inheritance but also leads to the variations through generations to ensure the evolutionary changes.[8] Henceforth, with precise vision toward the utmost importance of DNA reflects the dire need for its selective detection and localization inside cellular system as it can open up the new opportunities in various biological fields.[9-13] In this context, the fluorescence microscopy using suitable molecular stains has grown as a magnificent and effective tool for imaging various biomolecules and cell organelles mainly because of its non-invasive nature.[14-16] Real time analysis of bio-events using fluorescence microscopy requires longer hours visualization of biomolecules, and hence the whole process needs bright optical probe with good photostability inside living systems. Through decades of efforts a wide variety of fluorescent molecular stains bearing heterocyclic framework have been developed and used.[17-19] Despite of their availability, the poor selectivity, low biocompatibility and resistance toward photobleaching coupled with high phototoxicity are the consistent shortcomings of many developed stains which restrict their wide applicability.[20-22] Therefore, during formulation of their molecular architecture one should critically think about their three dimensional geometry and proper functional group orientation to construct a molecular probe of choice for selective binding with DNA to ensure its applicability for imaging and localization of DNA inside the cellular milieu.

In recent time, efforts are also being directed for developing G-quadruplexes selective probes for further biological applications. For example, Lu group developed and reported the structurally engineered thiazole orange for selective detection of telomeric G-quadruplexes.[23] Later, Zhang group reported a G-quadruplex selective indole-lutidnium based probe which was used for sensitive detection of uracil-DNA glycosylase activity.[24] The present work demonstrates the application of indole-lutidinium conjugate **P3** as a π-conjugated D-π-A^+-π-D sandwich type bright turn-on cationic molecular probe for selective detection and imaging of DNA inside cellular system. The probe showed much superior photobleaching resistance inside biological systems as compared to commercial stain Syto-16, indicating its potential as a photostable probe for longer duration fluorescence imaging of DNA inside cellular systems. Being itself non-fluorescent, background fluorescence has not been an issue while lighting up DNA with **P3**, and a significant enhancement in fluorescence intensity was observed upon complexation of **P3** with DNA. Moreover, **P3** was investigated to have low cytotoxicity and negligible phototoxicity. Combined theoretical and experimental studies revealed that strong fluorescence enhancement is possible only when the probe attains a suitable molecular geometry in the presence of suitable chemical functionality. To support this conclusion, a small library of five molecular probes **P1-P5** with tuned molecular architectures was synthesized, and their interactions with DNA were studied in detail.

Results and discussion

Synthesis of the molecular probes

The probes **P1-P5** were synthesized by adopting a three step synthesis procedure (see Scheme 1). In short, the lutidinium salt was synthesized in

[a] School of Basic Sciences, Indian Institute of Technology Mandi, Mandi-175001, H.P, India
[b] Department of Biophysics, Post Graduate Institute of Medical Education and Research, Chandigarh-160012, India

† Footnotes relating to the title and/or authors should appear here.
Electronic Supplementary Information (ESI) available: [details of any supplementary information available should be included here]. See DOI: 10.1039/x0xx00000x

View Article Online
DOI: 10.1039/C6TB00787B

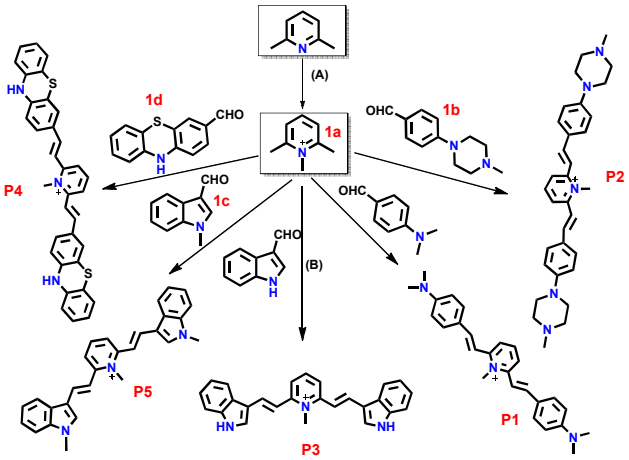

Scheme 1. Synthetic pathway of the probes (**P1-P5**). (A) DCM, MeI, RT; (B) Methanol, Piperidine, Reflux.

one step from 2, 6-lutidine followed by the Knoevenagel condensation between lutidinium salt and the corresponding aldehydes resulted in the formation of desired products.[25]

Photophysical properties

The optical response of the probes **P1-P5** toward DNA was examined under physiological conditions (10-X Tris-HCl, pH = 7.34, 25°C) employing absorption/emission spectroscopy. We started our investigations with **P1**/**P2** where both the probes were observed to be weakly fluorescent in Tris-HCl (λex = 465, 417 nm and λem = 634, 566 nm respectively), but upon addition of DNA only **P2** displayed a very little enhancement in fluorescence intensity, while no change in emission profile of **P1** was observed (see Fig. S1). After that, the probe **P3** (bearing indole as a donor with –NH group in the ring) was inspected to evaluate its photoresponse both in the presence and absence of DNA under similar set of conditions. The probe **P3** was

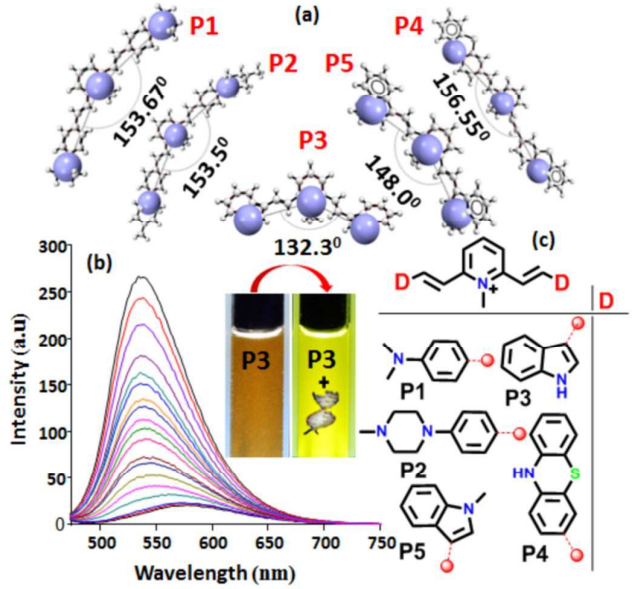

Fig. 1 a) ORTEP structures of the probes **(P1-P5)** showing curvature size, **b)** emission spectra of **P3** in presence of DNA (0 – 1mg/mL) and **c)** chemical architectures of the probes **(P1-P5).**

weakly fluorescent (ϕ = 0.0029) in buffer at λex = 447 nm (ϵ = 21400 M^{-1} cm^{-1}), while upon interaction with DNA, the probe **P3** displayed significant enhancement in its emission intensity (ϕ = 0.26 and ϵ = 29300 M^{-1} cm^{-1}) at λem = 537 nm and a bathochromic shift of 38 nm in absorption spectra. A large Stokes shift of 90 nm indicated the pseudo mega Stokes behaviour of **P3**.These optical responses of **P3** can be attributed to attainment of molecular planarity by the probe in the hydrophobic microenvironment of the minor groove of DNA that led to the freezing of its intramolecular rotation.[26-30] Further, the restricted intramolecular rotation of **P3** facilitated an efficient electronic delocalization through molecular planarity from indole to lutidinium. Moreover, the similar trends in the optical response of probe **P3** in glycerol (see Fig. S2) strengthened the dependence of **P3** toward the constraints of microenvironment (viscosity/minor groove interactions). The aforementioned optical responses of **P3** upon interaction with DNA prompted us also to understand the key structural features which predominantly govern the binding affinities of these probes toward DNA in the present study. After a careful structural inspection on **P1**-**P3**, it was speculated that either the geometric conformation/orientation of the probes or the presence of unrestricted –NH group in the heterocyclic system is the regulating factor for their response toward DNA. Further to validate the aforementioned speculation, probes **P4** (bearing phenothiazine with –NH group in ring system) and **P5** (bearing indole with –NMe group) were synthesized and their photophysical behaviour was studied under the similar conditions. Interestingly, **P4** was found to be almost non-fluorescent (λex = 519 nm, λem = 550 nm) both in the presence and absence of DNA (see Fig. S1) which clearly elucidated that the presence –NH group in the ring system is not the only key governing factor to show DNA binding affinity of these probes. In contrast, **P5** displayed slight enhancement (~2-folds) in its emission profile (λem = 562 nm) at λex = 452 nm upon interaction with DNA (see Fig. S1). This demonstrated that the precise orientation and geometry of its molecular architecture coupled with the presence of –NH group (either as an electron releasing group or as a hydrogen bonding site) could be the possible governing factor for the fluorescence enhancement and efficient binding of **P3** with DNA (Association constant = 6.5×10^4 M^{-1}). Moreover, from the aforementioned findings it was envisioned that the existence of hydrogen bonding, weak Vander Wall, pi-pi and electrostatic interactions may be the possible cause of probe-DNA complex formation. Furthermore, a careful literature survey revealed that indole has the structural resemblance with naturally occurring nuclear bases and this could also facilitate the interaction between **P3** and DNA as compared to other probes. [31-38] Next to evaluate the selectivity of **P3** as a DNA selective stain, its fidelity toward DNA detection was investigated in the presence of RNA and various types of proteins under similar set of conditions in solution phase. Interestingly, **P3** was found to exhibit more selectivity towards DNA (Limit of detection = 0.34 μM) as compared to other bioanalytes as shown in Fig. S5 and Fig. S6.

Theoretical studies to evaluate the molecular geometry of the probes

Next, the interaction behaviour of the probes (**P1**-**P5**) toward DNA was investigated by studies of density functional theory (DFT). Interestingly, the results of molecular simulations clearly indicated that the probes **P1**, **P2, P4** and **P5** exhibit stable conformations with small molecular curvatures (153.67°, 153.5°, 156.55° and 148.0° respectively) between two terminal heterocycles and the central lutidinium unit (see Fig. 1). On the basis of their curvature size, the non-interaction behaviour of **P1**, **P2** and **P4** with DNA was attributed to their little curved geometries closer to linearity. However, a little fluorescence enhancement in the case of **P5** is the clear indication of its more curved geometry as compared to **P1**, **P2** and **P4.** Interestingly, **P3** was found to be stable in its inherent semilunar conformation with curvature size of 132.3° that facilitated its proper binding in the minor groove of DNA.[39-45] The binding induced molecular planarity of **P3** further led to the efficient charge transfer between lutidinium (A^+) and indole (D) moieties through vinyl linkage (D-π-A^+-π-D system) upon interaction with DNA. Henceforth, the outcomes of simulation analysis strongly strengthened our assumption that the existence of **P3** in semilunar geometry equipped with free –NH group and structural resemblance of indole with natural nuclear bases led to its preferential interaction with DNA over other developed probes.

View Article Online
DOI: 10.1039/C6TB00787B

Furthermore, the molecular geometry of **P3** along with its HOMOs-LUMOs clearly illustrated that the molecular halves are spread over whole molecular framework that led to the extended conjugation length (see Fig. 2) and hence responsible for the charge transfer characteristic in its optical behaviour in the presence of DNA.

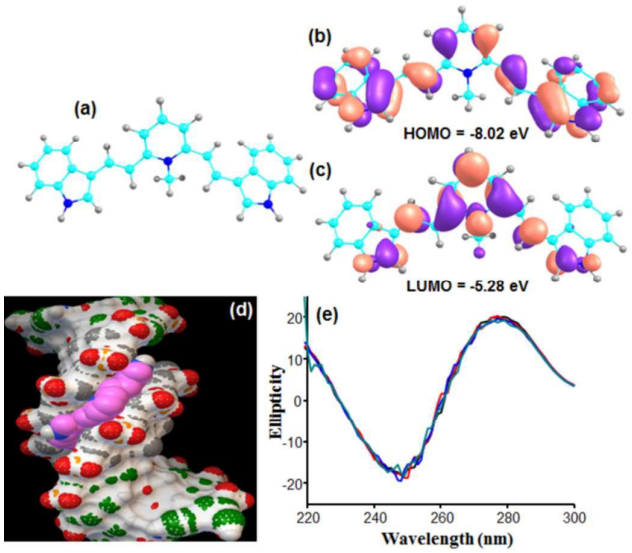

Fig. 2 a, b, c) The optimized geometry of **P3** with its HOMOs-LUMOs respectively, and **d, e**) optimized geometry of **P3-DNA** assemblage by molecular modelling and unchanged CD-spectra of DNA upon addition of **P3** (0 – 10 μM) respectively.

Molecular docking

Further, to specify the probe-DNA interactions, molecular modeling was performed using theoretically optimized geometry of **P3** with the help of Autodoc 4.2.[46] The findings of molecular modelling revealed the presence of pure electrostatic interactions in probe-DNA complex instead of weak π-π stacking and hydrogen bonding. The energetically optimized geometry of probe-DNA complex showing docking of **P3** specifically in Adenine-Thymine (A-T) rich assemblage of DNA is depicted in Fig. 2.

Circular dichroism

Next, to get deep insight into the of probe-DNA binding interactions as well as to evaluate the induced conformational variation in DNA helix, the structural ellipticity of DNA was examined in the presence of **P3** (0 – 10 μM) employing circular dichroism (CD) experiment. The CD spectra of Herring sperm DNA is characterized by a negative band at 245 nm and a positive band at 275 nm which is a characteristic of B-DNA.[47] Keeping the DNA concentration same (1 mg/mL), **P3** was added in three aliquots (2, 5 and 10 μM) to record the CD spectra. As illustrated in Fig. 2, the unperturbed positive and negative bands of DNA at 275 and 245 nm respectively established the existence of pure electrostatic interactions which supported the outcomes of molecular simulation.[30, 47]

Potential of P3 as fluorescent dye for nuclear staining

The appreciable findings of solution phase assays made us curious to explore the real applicability of **P3** toward molecular imaging and localization of DNA in cellular milieu employing HeLa cells. Both live and fixed cells were incubated with 10 μM of **P3** with and without permeabilization, and the images were acquired using Laser Scanning Confocal Microscope (model-IX81, version-3.0.2.0; Olympus) using Fluoview FV 1000 software. Probe **P3** was found to display an efficient and bright fluorescent staining of nucleus inside cells under both conditions. This not only reflected its unambiguous potential to stain both live and fixed cells, but also mirrored its quick cell membrane permeability (see Fig. 3 and Fig. S8) without the presence of any permeabilization agent. Fig. 3 clearly shows that the probe **P3** is efficient enough to induce bright optical signals

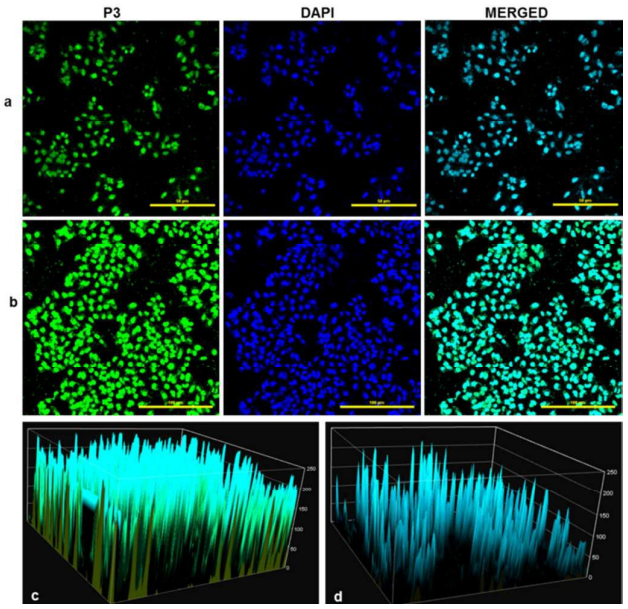

Fig. 3 Staining in fixed HeLa cells for 30 min **a**) with permeabilization, **b**) without permeabilization, **c**) intensity surface plot for condition **a** and **d**) intensity surface plot for condition **b.** Cells were incubated with **P3** (10 μM) for 30 min and **DAPI** (0.3 μM) for 5 min. Magnification 20x, scale bar 50 μm for permeabilized and 100 μm for cells without permeabilization.

(Brightness = 7.618 × 10^3 M^{-1} cm^{-1}) upon binding with the nuclei inside the fixed and live cells. Further to study the specificity towards DNA localization with its counter-labelled, the counterstain compatibility was evaluated and quantified using DNA-selective stain 4', 6-diamidino-2-phenylindole (DAPI) as a counterstain. As depicted in Fig. 3 and Fig. S10, the probe **P3** exhibited excellent counter stain compatibility in term of its negligible cytoplasmic spillage. The area of the nucleus stained by DAPI and **P3** were 7.3 ± 0.9 μm and 8.5 ± 1.6 μm respectively as quantitated by NIS elements provided as a software package with fluorescent microscope (see Fig. S10)**.** Moreover, the efficient nuclear imaging coupled with negligible change in cell morphology during visualization undoubtedly revealed its low cellular toxicity which is the prime requirement of a molecular probe to be used for cellular imaging. This was further supported by >92% cell viability of the incubated HeLa cells post 1 h (see Fig. S10).

Selectivity of P3 toward DNA in cellular system

Furthermore, to establish the selectivity of **P3** toward DNA inside the cells and to validate the outcomes of solution assay, deoxyribonuclease and ribonuclease (DNase/RNase) mediated experiments were conducted using **DAPI** as a control.[27] In the DNA digest test where DNA was digested by DNase (100 μg/mL, from Black Biotech) as per the expectation almost disappearance of fluorescence signal was noticed both in the case of **P3** as well as **DAPI** (see Fig. 4). In contrast, when RNA was digested using RNase (40 μg/mL, from MagGenome) the original fluorescence signal was found to be intact in the nucleus stained with **P3** and **DAPI** (see Fig. 4). The aforementioned findings not only validated the selectivity of **P3** toward DNA in solution but also established that the probe can be used as a selective nuclear stain for fluorescence imaging in the cellular system. Moreover, the binding potential of probe **P3** with cellular DNA in electrophoresis gel based system was also investigated. The strong binding of **P3** with DNA of β-actin displayed efficient staining but such staining was not observed after DNase digestion which again highlighted the high specificity of **P3** in gel as well (see Fig. S9).

Photobleaching tolerance and photo-induced toxicity investigations

Since, high photobleaching resistance and minimum photo induced toxicity are the mandatory criteria for a promising molecular probe to be used for fluorescence imaging inside the cellular milieu, [48-51] we became interested to

View Article Online
DOI: 10.1039/C6TB00787B

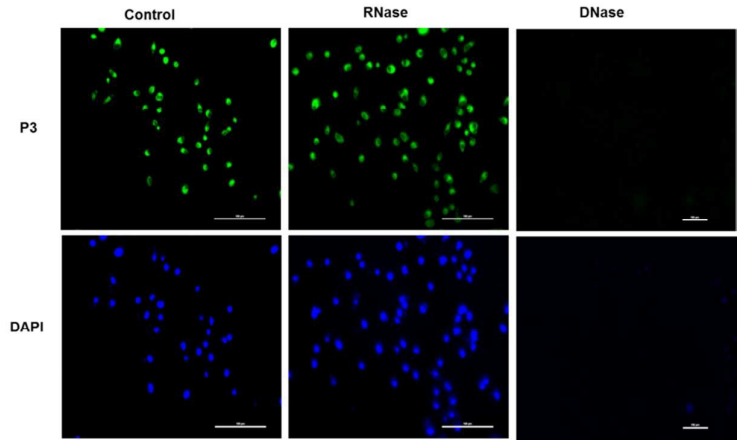

Fig. 4 Images of fixed HeLa cells in DNase/RNase digest tests. The cells were incubated with 10 µM of **P3** and (0.3 µM) **DAPI**. Upper panel shows P3 labeling in cells treated with PBS (control), RNase and DNase1. Lower panel shows DAPI as a positive control under similar conditions. Magnification 20x and scale bar-100 µm.

investigate its photostability inside cellular system. Fluorescent microscope was employed to evaluate and compare the photostability of **P3** with a known commercially available dye **Syto-16** inside the fixed HeLa cells. The cells were incubated with 10 µM **P3/Syto-16** and uninterruptedly exposed under 50 W mercury lamp (FITC-channel, 488 nm, 12×10^{19} photons/sec). It was quite exciting to observe that **Syto-16** lost its intensity within 2 min, whereas **P3** retained more than 30% of its initial fluorescence intensity even after 10 min of continuous illumination as depicted in Fig. 5 (all exposure parameters were kept same during photostability comparison). Hence, the photostability experiments established the admirable photostability of **P3** over **Syto-16**. Though the visible wavelength excitation and emission of **P3** abolished the chance of induction of phototoxicity during UV-exposure, the photo induced toxicity of a fluorescent probe under its own excitation maxima during cellular imaging cannot be ignored. Therefore, the promising findings of afore-performed bioassays encouraged us to evaluate the photoinduced toxicity of **P3** in cellular system. Amazingly, **P3** displayed negligible photoinduced toxicity (96.9% cell viability over 6 h as evidented by Fig. S10) during exposure under 488 nm light source (FITC-channel, 12×10^{19} photons/sec), which again supported its encouraging candidature as a promising nuclear stain for futuristic applications in the field of biomolecular imaging for longer period of exposure.

Conclusions

Hence to summarize, an indole-lutidinium conjugate **P3** with semilunar molecular framework and large curvature was investigated to have strong potential as a photostable and low cytotoxic molecular probe for fluorescence imaging of cellular nucleus, both in live and fixed cells. The probe **P3** is highly selective for DNA and has been noticed to induce negligible phototoxicity under continuous light exposure. The requirement of indole moiety along with -NH functionality and the importance of precise orientation of molecular architecture toward DNA binding were established employing solution phase assays followed by molecular simulation studies. The preferential and efficient binding with DNA as compared to other bioanalytes, and appreciable quantum efficiency coupled with promising brightness reflected the potent standing of **P3** as an important optical material. Moreover, it is worth mentioning that the admirable photostability under continuous exposure of light source coupled with minimal cytotoxicity and phototoxicity unambiguously enlightened the promising candidature of **P3** as a probable nuclear stain for the advanced studies of DNA molecular dynamics to successfully establish its utility in various biomedical fields.

Acknowledgements

Financial support was received from the Department of Science and Technology, India (Grant No. SERB/F/2408/2012-13). PG and AK are grateful to DST and CSIR for their fellowship. We thankfully acknowledge the Director, IIT Mandi for research facilities. Sophisticated instrument facility of Advanced Materials Research Center (AMRC), IIT Mandi, is thankfully acknowledged. We acknowledge Dr. Sougata Sinha and Mr. Sunil Kumar for their help during manuscript preparation.

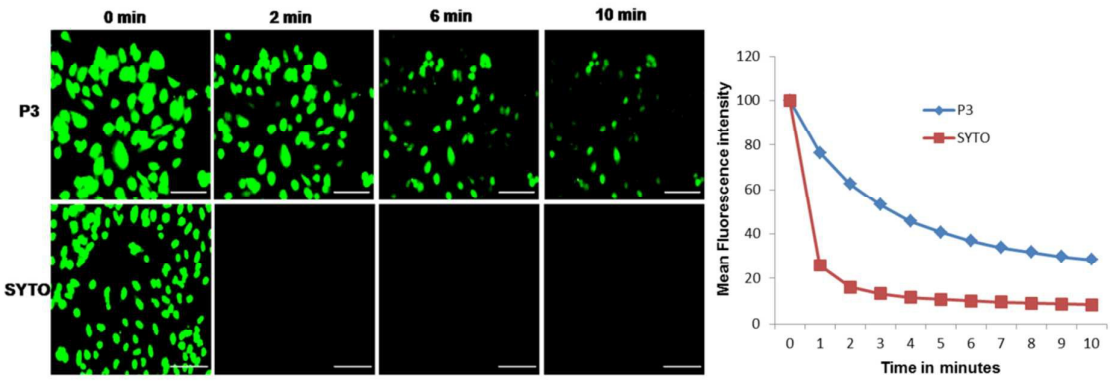

Fig. 5 Photostability of **P3** and **Syto-16**. Fluorescent microscopic images of HeLa cells post 2 h incubation with 10 µM **P3** and **Syto-16**. Graph showing the mean fluorescence intensity retained for both **P3** and **Syto-16** in fixed HeLa cells after 10 min of exposure. Fluorescence intensity of Images captured at 0 min was considered 100%. Images are representative images only. Magnification 20x, scale bar 100 µm.

View Article Online
DOI: 10.1039/C6TB00787B

Notes and References

1 N. K. Kaushik, N. Kaushik, P. Attri, N. Kumar, C. H. Kim, A. K. Verma and E. H. Choi, *Molecules (Basel, Switzerland)* 2013, **18**, 6620-6662.

2 R.G. Franzen, *J. Comb. Chem.* 2000, **2**, 195-214.

3 R. E. Dolle, *J. comb. chem.* 2001, **3**, 477-517.

4 S. Hanessian, G. McNaughton-Smith, H.G. Lombart and W.D. Lubell, *Tetrahedron* 1997, **53**, 12789–12854.

5 H.-A. Ho, A. Najari and M. Leclerc, *Acc. Chem. Res*. 2008, **41**, 168−178.

6 A. Granzhan and H. Ihmels, Org. Lett. 2005, **73**, 5119−5122.

7 V. P. Tokar, M. Y. Losytskyy, T. Y. Ohulchanskyy, D. V. Kryvorotenko, V. B. Kovalska, A. O. Balanda, I.M. Dmytruk, V. M. Prokopets, S. M. Yarmoluk and V. M. Yashchuk, *J. Fluoresc.* 2010, **20**, 865−872.

8 L. B. Jorde and S. P. Wooding, *Nat. Genet.* 2004, **36**, 28-33.

9 P. Zhang, T. Beck and W. Tan, *Angew. Chem. Int. Ed.* 2001, **40**, 402-405.

10 G. Ramsay, *Nat. Biotech.* 1998, **16**, 40-44.

11 J. Wang, *Nucleic Acids Res.* 2000, **28**, 3011-3016.

12 G. Hong, S. Diao, A. L. Antaris and H. Dai, *Chem. Rev.* 2015, **115,** 10816-10906.

13 M. Hegner and W. Grange, *J. Muscle Res. Cell Motil.* 2002, **23**, 367-375.

14 L. Ploeger, H. Dullens, A. Huisman and P. van Diest, *Histochem.* 2008, **83**, 63-69.

15 C. Holzhauser and H.-A. Wagenknecht, *Angew. Chem. Int. Ed.* 2011, **50**, 7268-7272.

16 C. Holzhauser, R. Liebl, A. Goepferich, H.-A. Wagenknecht and M. Breunig, *ACS Chem. Biol.* 2013, **8**, 890-894.

17 D. R. G. Pitter, J. Wigenius, A. S. Brown, J. D. Baker, F. Westerlund and J. N. Wilson, *Org. Lett.* 2013, **15**, 1330-1333.

18 N. I. Shank, H. Pham, A. S. Waggoner and B. A. Armitage, *J. Am. Chem. Soc.* 2013, **135**, 242-251.

19 M. M. Rubner, C. Holzhauser, P. R. Bohländer and H.-A. Wagenknecht, *Chem. Eur. J.* 2012, **18**, 1299-1302.

20 S. K. Yang, X. Shi, S. Park, T. Ha and S. C. Zimmerman, *Nat. Chem.* 2013, **5**, 692-697.

21 E. B. Veale, D. O. Frimannsson, M. Lawler and T. Gunnlaugsson, *Org. Lett.* 2009, **11**, 4040-4043.

22 G. P. Pfeifer and Y.-H. A. You, *Mutat. Res. Fund. Mol. Mech. Mut.* 2005, **571**, 19-31.

23 Y.-J. Lu, Q. Deng, J.-Q. Hou, D.-P. Hu, Z.-Y. Wang, K. Zhang, L. G. Luyt, W.-L. Wong and C.-F. Chow, *ACS Chem. Biol.* 2016. DOI: 10.1021/acschembio.5b00987

24 Y.-J. Lu, D.-P. Hu, Q. Deng, Z.-Y. Wang, B. H. Huang, Y. X. Fang, K. Zhang and W.-L. Wong, *Analyst* 2015, **140**, 5998-6004.

25 F. Yang, X.-L. Xu, Y.-H. Gong, W.-W. Qiu, Z.-R. Sun, J.-W. Zhou, P. Audebert and J. Tang, *Tetrahedron* 2007, **63**, 9188-9194.

26 S. Ghosh, D. Banik, A. Roy, N. Kundu and J. Kuchlyan, *Phys. Chem. Ch. Ph.* 2014, **16**, 25024-25038.

27 N. Narayanaswamy, M. Kumar, S. Das, R. Sharma, P. K. Samanta, S. K. Pati, S. K. Dhar, T. K. Kundu and T. A Govindaraju, *Sci. Rep.* 2014, **4**,1-10.

28 X. J. Feng, P. L. Wu, F. Bolze, H. W. C. Leung, K. F. Li, N. K. Mak, D. W. J. Kwong, J.-F. Nicoud, K. W. Cheah and M. S. Wong, *Org. Lett.* 2010, **12**, 2194-2197.

29 J. Cao, C. Hu, F. Liu, W. Sun, J. Fan, F. Song, S. Sun and X. Peng, *Chem. Phys. Chem.* 2013, **14**, 1601-1608.

30 B. Dumat, G. Bordeau, E. Faurel-Paul, F. Mahuteau-Betzer, N. Saettel, G. Metge, C. Fiorini-Debuisschert, F. Charra and M.-P. Teulade-Fichou, *J. Am. Chem.Soc.* 2013, **135**, 12697-12706.

31 D. Loakes, D. Brown M. *Nucleic Acids Res.* 1994, **22**, 4039-4043.

32 K. Wang, S. Stringfellow, S. Dong and H. Yu, *Spectrochim. Acta. A Mol. Biomol. Spectrosc.* 2002, **58**, 2595-2603.

33 J. Barbaric, C. Wanninger-Weiß and H.-A. Wagenknecht, *Euro. J. Org. Chem.* 2009, **2009**, 364-370.

34 N. S. Girgis, H. B. Cottam and R. K. Robins, *J. Heterocyclic Chem.* 1988, **25**, 361-366.

35 J. S. Lai and E. T. Kool, *J. Am. Chem. Soc.* 2004, **126**, 3040-3041.

36 S. Moran, R. X. Ren, C. J. Sheils, S. Rumney and E. T. Kool, *Nucleic Acids Res.* 1996, **24**, 2044-2052.

37 S. Matsuda, A. A. Henry, P. G. Schultz and F. E. Romesberg, *J. Am. Chem. Soc.* 2003, **125**, 6134-6139.

38 D. Guianvarc'h, J.-L. Fourrey, M.-E. Tran Huu Dau, V. Guérineau and R. Benhida, *J. Org. Chem*. 2002, **67**, 3724-3732.

39 F. E. Wolter, K. Schneider, P. B. Davies, E. R. Socher, G. Nicholson, O. Seitz and R. D. Süssmuth, *Org. Lett.* 2009, **11**, 2804-2807.

40 M. L. Kopka, C. Yoon, D. Goodsell, P. Pjura and R. E. Dickerson, *J. Mol. Biol.* 1985, **183**, 553-563.

41 P. B. Dervan and B. S. Edelson, *Curr. Opin. Struc. Biol.* 2003, **13**, 284-299.

42 K. A. Muzikar, J. L. Meier, D. A. Gubler, J. A. Raskatov and P. B. Dervan, *Org. Lett.* 2011, **13**, 5612-5615.

43 A. Denisiuk, V. Schubert, F. E. Wolter, E. Irran, P. Trouillas, and R. D. Süssmuth, *Bioorg. Med. Chem.* 2013, **21**, 3582-3589.

44 X. Yue, Z. Armijo, K. King, M. V. Bondar, A. R. Morales, A. Frazer, I. A. Mikhailov, O. V. Przhonska and K. D. Belfield, *ACS Appl. Mater. Interfaces* 2015, **7**, 2833-2846.

45 P. S. Nagle, C. McKeever, F. Rodriguez, B. Nguyen, W. D. Wilson and I. Rozas, *J. Med. Chem.* 2014, **57**, 7663-7672.

46 S. Hanlon, S. Brudno, T. T. Wu and B. Wolf, *Biochem.(Mosc).*1975, **14**, 1648-1660

View Article Online
DOI: 10.1039/C6TB00787B

47 G. M. Morris, D. S. Goodsell, R. S. Halliday, R. Huey, W. E. Hart, R. K. Belew and J. Olson, *J. Comput. Chem.* 1998, **19**, 1639-1662.

48 P. R. Bohlander and H.-A. Wagenknecht, *Org. Biomol. Chem.* 2013, **11**, 7458-7462.

49 R. B. Peggy and H.-A. Wagenknecht, *Methods Appl. Fluores.* 2015, **3**, 044003.

50 M. Dyba and S. W. Hell, *Appl. Opt.* 2003, **42**, 5123-5129.

51 G. Lukinavicius, C. Blaukopf, E. Pershagen, A. Schena, L. Reymond, E. Derivery, M. Gonzalez-Gaitan, E. D/'Este, S. W. Hell, D. Wolfram Gerlich and K. Johnsson, Nat.Commun. 2015, **6**, 1-7.